Available online at www.sciencedirect.com
ScienceDirect
Journal of Solid State Chemistry 180 (2007) 84–91
JOURNAL OF SOLID STATE CHEMISTRY
www.elsevier.com/locate/jssc

On α–β phase transition in cristobalite-type $Al_{1-x}Ga_xPO_4$ $(0.00 \leqslant x \leqslant 1.00)$

S.N. Achary, R. Mishra, O.D. Jayakumar, S.K. Kulshreshtha, A.K. Tyagi*

Chemistry Division, Bhabha Atomic Research Centre, Mumbai-400 085, India

Received 4 April 2006; received in revised form 24 September 2006; accepted 26 September 2006
Available online 28 September 2006

Abstract

The results of variable temperature powder X-ray diffraction and differential thermal analysis (DTA) studies on the orthorhombic (α) low-cristobalite to cubic (β) high-cristobalite phase transition for $Al_{1-x}Ga_xPO_4$, $(0.00 \leqslant x \leqslant 1.00)$ are presented. These studies reveal that all these compositions undergo reversible phase transitions from orthorhombic to cubic form at higher temperature. The high-temperature behavior of $GaPO_4$ is observed to have a different behavior compared to all other compositions in this series. Orthorhombic low-cristobalite-type $GaPO_4$ transforms to cubic high-cristobalite form at ~605 °C. Above ~700 °C, the cubic high-cristobalite-type $GaPO_4$ slowly transforms to trigonal quartz type structure. At about 960 °C, the quartz type $GaPO_4$ transforms back to the cubic high-cristobalite form. During cooling cycles the cubic phase of $GaPO_4$ reverts to trigonal quartz type phase. However, annealing of $GaPO_4$ at higher temperatures for longer duration can stabilize the orthorhombic low cristobalite phase. The phase transition temperatures and associated enthalpies are related to the change in unit cell volume and the orthorhombicity of the respective low cristobalite lattice.

Keywords: Cristobalite; Phosphate; Phase transition; DTA; HT-XRD

1. Introduction

Crystalline materials with corner-linked polyhedral structures have drawn considerable interest in recent years owing to their structural flexibility leading to different structural modifications under various non-ambient conditions. Such structural architect is often categorized as framework structure. Several silicates, phosphates, molybdates, tungstates are known to have such framework-type polyhedral structures [1–4]. The crystal structure of SiO_2 has similar framework arrangements where the SiO_4 tetrahedra share their corners forming a three dimensional network [5]. Depending on temperature, SiO_2 undergoes various reconstructive phase transitions to give quartz, tridymite and cristobalite structures. In addition within a given polymorph they undergo various displacive-type phase transitions [5]. Several phosphates of trivalent cations crystallize in various silica analog structure types. $AlPO_4$ and $GaPO_4$ are such examples where all the ambient pressure (1 atm) silica polymorphs have been reported [5–17]. The structural topology of $AlPO_4$ and $GaPO_4$ are essentially same as that of SiO_2 except the cation (M and P) orderings leading to different symmetry in phosphates compared to SiO_2. The different polymorphs of these phosphates formed by reconstructive phase transitions can be retained at ambient temperature (25 °C) by optimizing the preparation conditions, like, high-temperature quench method or long annealing above the phase transition temperature. For both $GaPO_4$ and $AlPO_4$ the cristobalite-type phases are reported at higher temperatures. The low cristobalite (orthorhombic) phase can be retained by annealing above 1300 °C for 24 h and cooling at about 500 °C/h or by removing from furnace to room temperature in air [18–20]. Though, different polymorphs of $AlPO_4$ and $GaPO_4$ have been known from long days, the systematic structural studies with composition as well as with pressure and temperature are relatively scarce. The temperature and pressure variation of crystal structures of quartz-type $AlPO_4$ and $GaPO_4$ have been reported in

*Corresponding author. Fax: +91 22 25505151.
E-mail address: aktyagi@barc.ernet.in (A.K. Tyagi).

0022-4596/$ - see front matter © 2006 Elsevier Inc. All rights reserved.
doi:10.1016/j.jssc.2006.09.017

literature [10–17,20–25]. Goiffon et al. [12] have reported the crystal structure of these quartz-type phosphates at low temperature (down to 173 K). No structural transformation except the unit cell contraction and reduction of the amplitude of thermal vibrations has been observed at lower temperature. Later, Worsch et al. [23,24], Nakae et al. [13], Haines et al. [15–17], Kosten and Arnold [25], Jacob et al. [26] have studied the details of the phase transition of the quartz-type $GaPO_4$ and $AlPO_4$. In these studies, the thermal expansion behaviors in a wider range of temperature have been reported. Also, the quartz to high-cristobalite transformation for $GaPO_4$ at around 960 °C has been reported. Although, several reports pertaining to the high temperature behavior of quartz-type phosphates exist, only a few reports dealing with the cristobalite-type phosphates are available in literature. Ng and Calvo [27] have studied the low to high-cristobalite structural transformation and thermal expansion details of $AlPO_4$. Hatch et al. have [28] studied the low to high-cristobalite transformation and their symmetry relations. Earlier, we have reported [20] the detailed structural variation of low and high-cristobalite-type $AlPO_4$ and $GaPO_4$ with temperature as well as compositions. The formation of perfectly random solid solution between the low cristobalite-type $AlPO_4$ and $GaPO_4$ phases have been confirmed from ^{31}P NMR, powder X-ray diffraction (XRD) as well as neutron diffractions [19,20,29]. No structural change or phase segregation at lower temperature (down to 15 K) has been observed in similar mixed phosphates [30]. In all these studies the crystal structures the high-cristobalite $AlPO_4$ or $GaPO_4$ have been explained with a disordered anion sub-lattice. Recently, the disordered anion sub-lattice of the high-cristobalite is confirmed by neutron scattering as well as reverse Monte-Carlo studies [22]. Further, based on high temperature XRD studies, a significant decrease in thermal expansion coefficient was observed for the high-cristobalite-type structures compared to that of the low cristobalite-type structure. In contrast to other compositions, $GaPO_4$ exhibit an unusual behavior with the existence of trigonal quartz-type phase along with the cubic high-cristobalite phase at higher temperature [20]. The present study is aimed to understand the effect of composition on the nature of low- to high-cristobalite phase transition for $Al_{1-x}Ga_xPO_4$ samples and to evaluate the thermodynamic parameters associated with this phase transition in addition to provide further thermodynamic evidence of the unusual behavior of $GaPO_4$.

2. Experimental

The $Al_{1-x}Ga_xPO_4$ ($0.0 \leqslant x \leqslant 1.0$) compositions were prepared by the procedure reported earlier [19,20]. The colorless prepared samples were characterized by powder XRD patterns recorded on a Philips X-Pert pro Powder X-ray diffractometer equipped with a platinum strip heater using Cu$K\alpha$ ($K\alpha1 = 1.5406$ and $K\alpha2 = 1.5444$ Å) radiation. For high-temperature diffraction data the sample was heated to a desired temperature and then the XRD patterns were recorded in the two theta range of 10–80° with step width of 0.02° and step time of 0.8 s. The differential thermal analysis (DTA) scans were recorded on a Setaram simultaneous TG-DTA instrument model TG-DTA 92-16. For DTA study, about 50 mg of sample was filled in a platinum cup and heated at the rate of 10 °C/min. The enthalpy of phase transition for all these compositions was calculated from the area under the peak in DTA plots. For determination of the enthalpy change, the instrument was calibrated by measuring the heat of phase transformations of standard samples [i.e. KNO_3 (128 °C), $KClO_4$ (299 °C), Quartz (573 °C), K_2SO_4 (583 °C), $BaCO_3$ (810 °C)] under identical experimental conditions. The values of calibration constant K, determined at different temperatures for these standard compounds, was fitted into a polynomial equation. This equation was used to determine the values of K at transition temperature.

3. Results and discussion

From the room temperature powder XRD patterns (Fig. 1), the low-cristobalite (orthorhombic) lattice is confirmed for all these compositions. The close similarity of the XRD patterns of the mixed phosphate compositions with that of $AlPO_4$ and $GaPO_4$ suggests the formation of solid solution over the complete range of composition. The ideal solid solution in $AlPO_4$ and $GaPO_4$ is expected due to the similar structure and comparable ionic radii of Al^{3+} and Ga^{3+} (radii of Al^{3+} and Ga^{3+} for the tetrahedral coordination are 0.53 and 0.62 Å, respectively). The unit cell parameters of all the phases are obtained from Rietveld refinement of the observed profiles using Fullprof 2000 software package [31]. The Rietveld refinements are carried out with the initial structural parameters and the space group ($C222_1$) reported for the low-cristobalite-type $AlPO_4$ and $GaPO_4$ [18]. The observed unit cell parameters (Table 1) for $AlPO_4$ and $GaPO_4$ at room temperature are in agreement with the values reported in the literature [18,20,27,32]. The refined values of unit cell parameters for all these compositions along with the reported values of unit cell parameters of the end members, $AlPO_4$ and $GaPO_4$, are given in Table 1.

The crystallographic nature of the phase transitions for $Al_{1-x}Ga_xPO_4$ samples at higher temperatures as revealed by high-temperature XRD have been reported earlier [20]. The XRD patterns recorded after the phase transition temperature showed the formation of cubic high-cristobalite-type phases (Space Group: $F\bar{4}3m$), similar to the earlier reported studies for $AlPO_4$ [27]. The transformation from low-cristobalite to high-cristobalite is brought about by a cooperative displacement of AlO_4/GaO_4 and PO_4 tetrahedra forming more symmetric arrangements. A typical Rietveld refinement plot indicating the high-cristobalite-type phase for a representative composition ($Al_{0.2}Ga_{0.8}PO_4$) is shown in Fig. 2.

The orthorhombic to cubic transition for all the $Al_{1-x}Ga_xPO_4$ compositions appear as endothermic peak

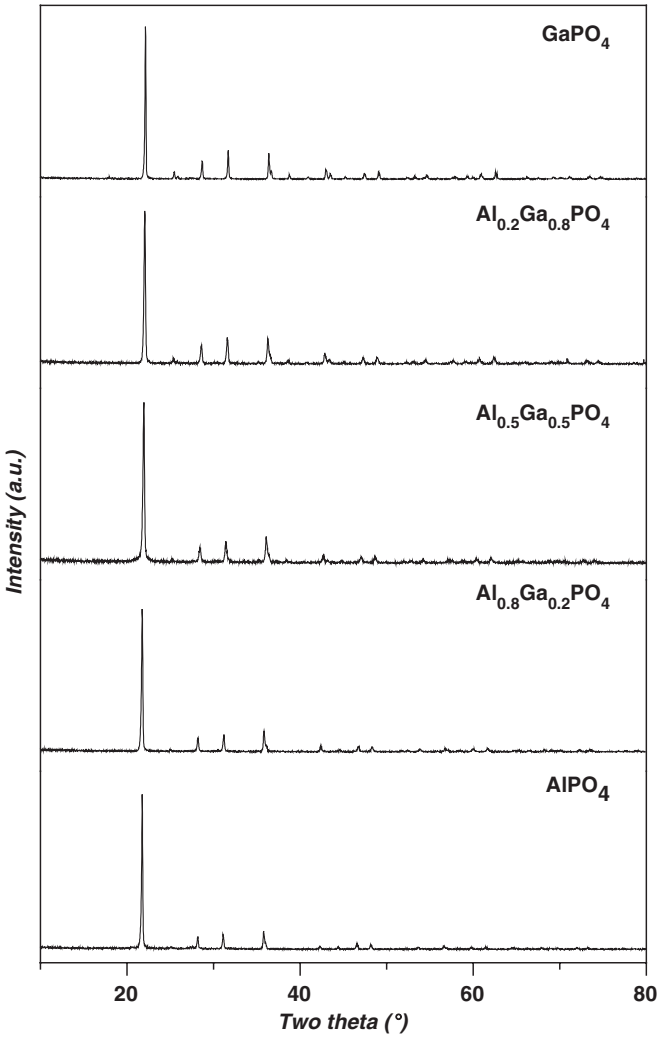

Fig. 1. Powder XRD patterns of $Al_{1-x}Ga_xPO_4$ samples at 25 °C exhibiting orthorhombic structure.

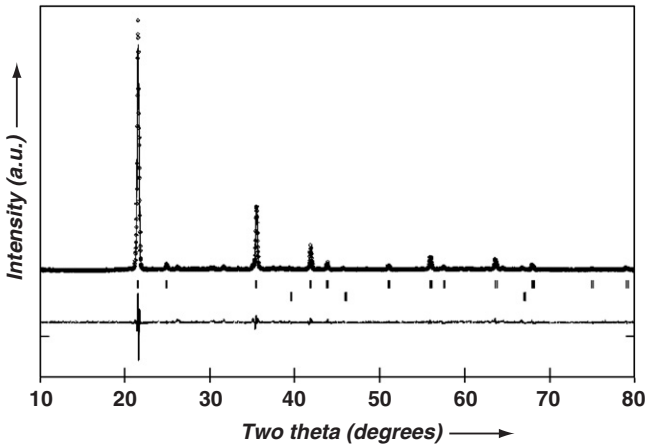

Fig. 2. Rietveld refinement plot for $Al_{0.2}Ga_{0.8}PO_4$, showing cubic high-cristobalite-type phase (pattern recorded at 600 °C). The platinum base metal peaks are shown as lower vertical bars.

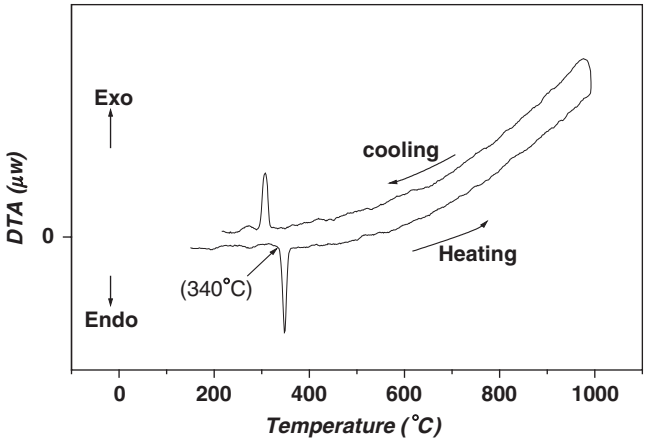

Fig. 3. DTA plot for $Al_{0.5}Ga_{0.5}PO_4$.

Table 1
Refined unit cell parameters for the room temperature phase of $Al_{1-x}Ga_xPO_4$ (crystal system: orthorhombic ($C222_1$))

	a (Å)	b (Å)	c (Å)	V (Å^3)	$D^a \times 10^4$	Ref.
$AlPO_4$	7.084(1)	7.082(1)	6.9989(4)	351.2(1)	1.4	
	7.099(2)	7.099(2)	7.006(2)	353.1(2)		[10]
	7.082	7.098	6.993	351.52		[16]
	7.078(2)	7.078(2)	6.991(2)	350.2(2)		[17]
$Al_{0.8}Ga_{0.2}PO_4$	7.053(1)	7.056(1)	6.9551(3)	346.1(1)	2.1	
$Al_{0.5}Ga_{0.5}PO_4$	7.030(1)	7.017(1)	6.9219(5)	341.4(1)	9.2	
	7.0295(8)	7.0132(8)	6.9187(4)	341.08(6)		[18]
$Al_{0.2}Ga_{0.8}PO_4$	6.997(1)	6.979(1)	6.8884(3)	336.4(1)	12.8	
$GaPO_{4a}$	6.987(1)	6.962(1)	6.8774(4)	334.6(1)	17.9	
	6.967	6.967	6.866	333.3		[10]

[a]D = orthorhombicity defined as $|(b-a)/(b+a)|$.

during the heating cycle. A typical DTA plot for mid-composition $Al_{0.5}Ga_{0.5}PO_4$ is shown in Fig. 3. In cooling cycle, the exothermic peak due to the transformation of high-cristobalite lattice to low-cristobalite lattice is observed at relatively lower temperature then the corresponding endothermic peak in heating cycle. This small thermal hysteresis for the phase transition is observed in each sample. The disordered structure of the high-cristobalite lattice is a subject of controversy and is attributed to highly disordered oxygen atoms of the MO_4 and PO_4 tetrahedra [20,22,27]. Attempts to stabilize the high-cristobalite structure at ambient temperature are not successful. This can be attributed to the drastic increase in molar volume at phase transition and highly disordered lattice of high-cristobalite, which differed by a small displacement of cations from the stable low-cristobalite lattice. The crystallographic as well as thermodynamic studies support for the first order transformation in these compositions. The thermal hysteresis in first order transformations is a common observation, where the superheating and supercooling and possible coexistence of both phases near the phase transition temperature is known [33–35]. Usually, such phase transformations occur with heterogeneous nucleation at the lattice defects. The strains introduced in the unit cell renormalize to give the long range structure of transformed phase in a wider temperature range [33–36]. The local stress around the nucleus leads to the possible

existence of the both phase in the vicinity of the transformation temperature. The hysteresis in displacive transformation in several of such compounds, like, $AlPO_4$, $GaPO_4$, SiO_2, etc., silicates, various perovskite-type solid solutions and super ionic materials undergoing first-order transformation have been reported under high-pressure or high-temperature conditions [33–42]. The micro-strain leading to twinning of the crystal is common known phenomena in $AlPO_4$, $GaPO_4$ [27]. In this sort order-disorder coupled displacive transitions, the main contributing factors towards the phase transition are related to micro- and macro-strain [43–45]. The internal strain present in the cooled sample may be a possible reason for the thermal hysteresis. This aspect is further explained in the later part of this manuscript. Besides, the thermal hysteresis may also appear from the experimental factors, like, packing of the sample in crucible as well as sintering of the sample after the heat treatment and thermal conductivity due to the difference in the mode of energy dissipation.

The enthalpy change accompanying the phase transition is estimated from the area under the peak. The values of enthalpy of phase transition and the onset temperatures for phase transition are given in Table 2. It is observed that the phase transition onset temperature as well as the enthalpy of phase transition for these compositions gradually increases with increasing Ga^{3+} contents. The low-cristobalite-type $GaPO_4$ shows the presence of a second phase transition at about 960 °C during heating cycle as seen in Fig. 4.

The earlier high-temperature XRD studies [20] also indicated that the high-temperature behavior of $GaPO_4$ is different from the rest of the compositions. The XRD results of $GaPO_4$ at 700 °C showed the existence of only cubic high-cristobalite-type phase. However, the XRD patterns recorded at still higher temperature, namely, 800 and 900 °C, show the presence of both trigonal quartz-type and cubic high-cristobalite-type $GaPO_4$ phases. This suggests that above 700 °C, the high-cristobalite-type $GaPO_4$ relaxes to trigonal quartz-type structure. This can be attributed to the higher molar volume of the cristobalite lattice compared to the quartz-type lattice of $GaPO_4$.

Table 2
Details of phase transformation as obtained from DTA for $Al_{1-x}Ga_xPO_4$

S. no.	Sample	Peak onset temp. (°C)	Peak temp. (°C)	Enthalpy of transition (kJ/mol)	$(\Delta V)^a$ (Å^3)
1	$AlPO_4$	202	213	1.67	15.2
2	$Al_{0.8}Ga_{0.2}PO_4$	273	280	2.36	15.4
3	$Al_{0.5}Ga_{0.5}PO_4$	340	348	3.00	19.7
4	$Al_{0.2}Ga_{0.8}PO_4$	506	529	6.14	21.6
5	$GaPO_4$	605	613	6.64	24.8

[a]Values of ΔV have been obtained by extrapolating the unit cell parameters of both orthorhombic and cubic phases up to the onset temperature of phase transition. (errors: temperature is ±2 °C, enthalpy of transition is about ±0.05 kJ/mol ΔV is ±0.2 Å^3).

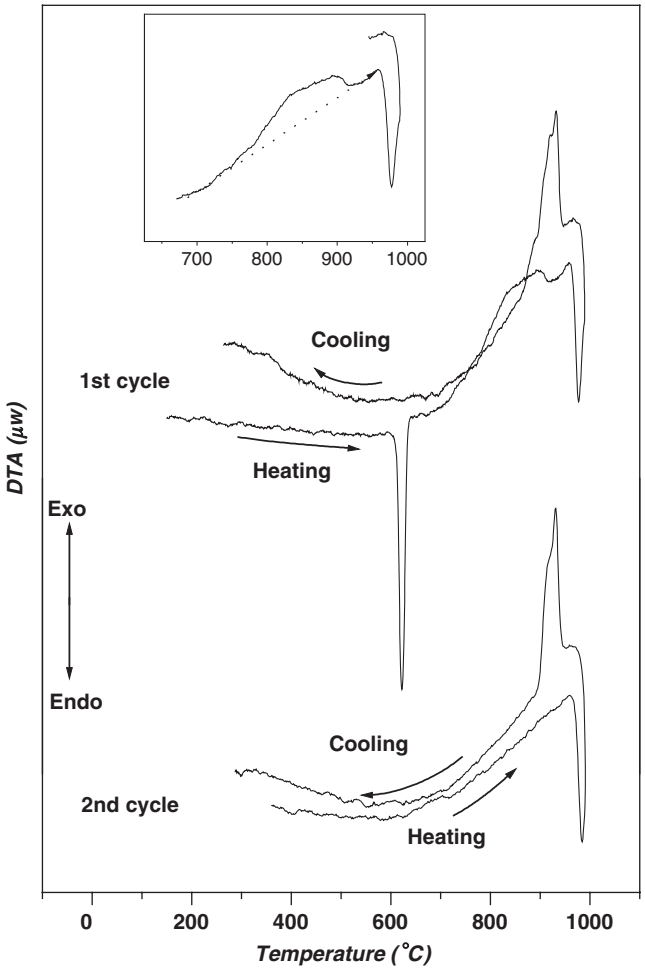

Fig. 4. DTA plot for cristobalite-type $GaPO_4$ (inset shows the a broad exotherm due to the relaxation of cristobalite to quartz-type $GaPO_4$).

The DTA scan of the $GaPO_4$ shows two endotherms (at 605 and 960 °C) corresponding to the low-cristobalite to high-cristobalite and quartz to high-cristobalite phase transformations. From the inset shown in Fig. 4, it is clearly seen that there is a significant deviation in the baseline above 700 °C. This broad exothermic peak can be attributed to the slow transformation of cubic phase to the trigonal form. The next endothermic peak at ~960 °C corresponds to the transformation of the trigonal quartz-type phase to the cubic high-cristobalite form. The XRD pattern recorded at 1000 °C shows the presence of only cubic phase, which is attributed to the transformation of trigonal quartz-type phase to high-cristobalite-type phase. Earlier, Kosten and Arnold [25] and Jacobs et al. [26] have reported the transformation of trigonal quartz-type $GaPO_4$ to cubic high-cristobalite lattice at about 933 °C [25,26]. During reverse cycle, i.e., cooling from 1050 °C only the cristobalite to quartz transformation was observed, indicating the formation of the quartz-type phase in cooled sample. This observation is confirmed on the second heating cycle in the DTA runs (Fig. 4), where the quartz to high-cristobalite transformation is reproduced. The powder XRD analysis of the DTA residue obtained after

cooling up to room temperature shows the formation of the quartz-type $GaPO_4$.

For comparison, the DTA runs recorded for the trigonal quartz-type sample, indicating the quartz to high-cristobalite transformation at 960 °C is shown in Fig. 5. It may be appropriate to mention that in the cooling cycle the exotherm, corresponding to the transformation of high cristobalite to quartz phase consists of two peaks with unequal intensity (Figs. 4 and 5). Such behavior can be observed if the high-cristobalite phase transforms to the quartz-type structure through an intermediate phase. In fact, the corresponding DTA endothermic peak in the heating cycle for quartz type $GaPO_4$ is also asymmetric in nature, implying the possible occurrence of an intermediate phase, which is unidentifiable at this stage.

From the high-temperature XRD studies it is observed that the fraction of trigonal quartz phase of $GaPO_4$ increased with increasing temperature of annealing. A quantitative analysis of the powder XRD patterns of cristobalite-type $GaPO_4$ recorded at 800 and 900 °C indicates the presence of 39.3(5) and 56.6(6) wt% of quartz-type $GaPO_4$. Thus, the exact ratio of the two phases depends on temperature and duration of annealing. The typical observed and calculated XRD patterns of $GaPO_4$ at 800 and 900 °C are shown in Figs. 6 and 7, respectively. From both the DTA and high-temperature XRD studies it can be concluded that the transformation of high cristobalite to quartz phase in $GaPO_4$ depends on temperature and duration of heating. On cooling the sample from high temperature, the high-cristobalite phase is completely transformed to trigonal quartz type phase, which is consistent with the earlier HT-XRD studies. These observations imply that the quartz-type $GaPO_4$ has higher stability than low and high-cristobalite forms of $GaPO_4$. However, annealing for longer time at well above quartz to high-cristobalite transformation temperature can retain the cristobalite [20]. Besides, the substitution of Ga^{3+} by Al^{3+} also inhibits the high-cristobalite to quartz transformation.

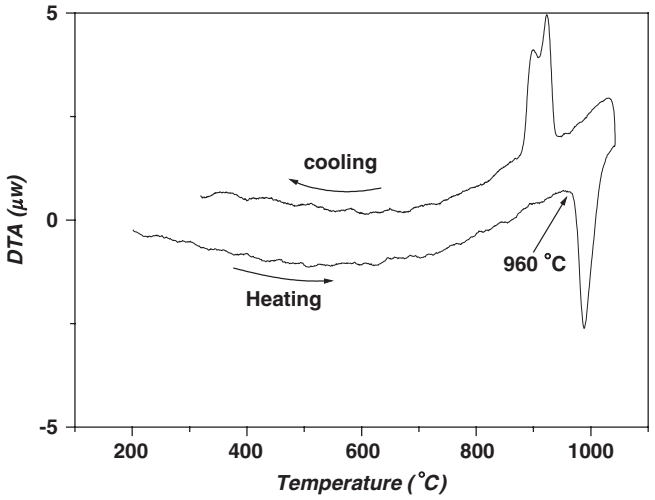

Fig. 5. DTA plot for quartz-type $GaPO_4$.

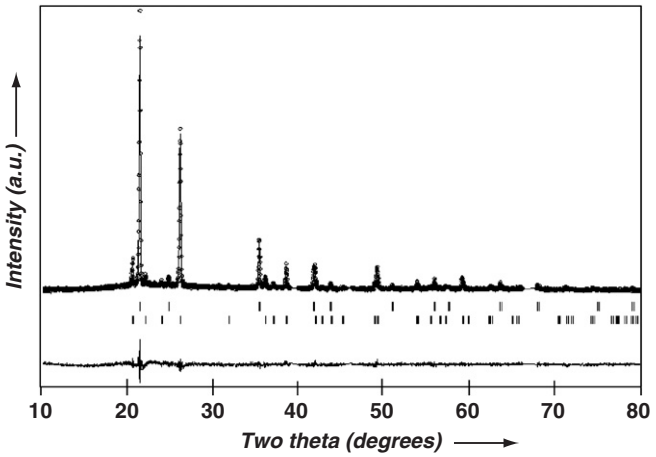

Fig. 6. Rietveld refinement plot for $GaPO_4$ at 800 °C, showing both high cristobalite (upper vertical mark) and quartz-type phase (lower vertical mark), platinum peaks are excluded in this refinement.

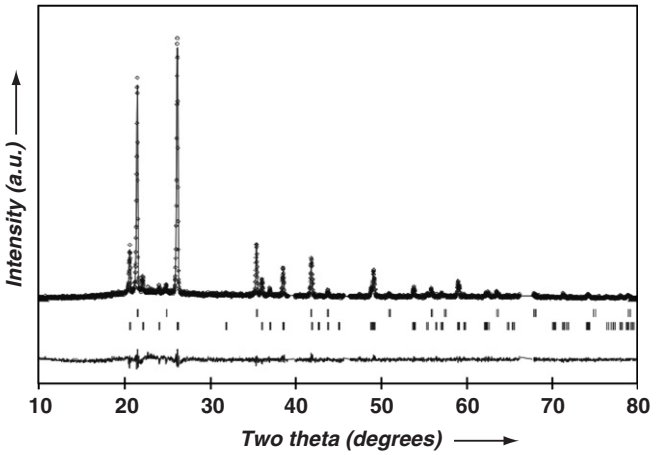

Fig. 7. Rietveld refinement plot for $GaPO_4$ at 900 °C, showing both high cristobalite (upper vertical mark) and quartz type phase (lower vertical mark), platinum peaks are excluded in this refinement.

The low cristobalite to high-cristobalite transformation temperature as well as enthalpy of transformation show a gradual variation with the composition (Table 2). A systematic variation of the crystal structure with composition has been explained in our earlier communication [20]. A comparison of the present data with the crystal structure details of these compositions implies that the variation of phase transformation temperature is a consequence of the change of crystal structure, in particular the M–O–P angle. It is observed that the unit cell volume of the orthorhombic (low-cristobalite) lattice decreases gradually with the increase in Ga^{3+} contents. In addition, the thermal expansion coefficient of orthorhombic lattice decreases from $AlPO_4$ to $GaPO_4$ and for the cubic lattice it increases from $AlPO_4$ to $GaPO_4$ [20]. It is also reported that this phase transformation is associated with drastic increase in molar volume. The change in unit cell volume (ΔV; excess volume) at the phase transformation temperature is obtained by extrapolating the unit cell

volume of the high-temperature and low-temperature phases to the exact transition temperature. The change in unit cell volume (ΔV) for the different compositions at the phase transformation temperature is listed in Table 2. It is observed that larger the value of ΔV, higher is the transition temperature as well as enthalpy of transition. The typical variation of the transition temperature, excess volume as well as enthalpy of transformation as a function of $GaPO_4$ content are shown in Fig. 8. Besides, the orthorhombicity of the low cristobalite phase can be correlated to the transition temperature as well as the enthalpy change associated with the phase transformation. The derived values of orthorhombicity for various compositions are listed in Table 1. The smaller value of observed orthorhombicity in $AlPO_4$ results in lower value of enthalpy and temperature of phase transition. It can be mentioned here the transition temperature and enthalpy of transition are related to the micro-strain in the transformation, which is mentioned later.

Earlier, a close correlation between the M–O–P bond angles and values of thermal expansion coefficients of the various compositions was reported [20,46]. Remarkably, a similar close correlation between the M–O–P angle and the phase transition temperature as well as the associated enthalpy change is observed. The M–O–P bond angles of various compositions at a particular temperature systematically decrease with the increase in Ga^{3+} contents. The average M–O–P bond angles for room temperature phases are 145, 142, 139, 137 and 133°, respectively, for $x = 0$, 0.20, 0.50, 0.80 and 1.00 compositions of $Al_{1-x}Ga_xPO_4$. The M–O–P bond of the cubic phase of the corresponding compositions are 147 (at 300 °C), 144 (at 400 °C), 142 (at 400 °C), 140° (at 600 °C) and 138° (at 700 °C) [20]. For $GaPO_4$ this angle changes from 133° (at RT, orthorhombic) to about 138° (at 700 °C, cubic), whereas in case of $AlPO_4$ the change is from 145° (at RT, orthorhombic) to 147° (at 300 °C, cubic) [20]. These facts indicate that the structure of orthorhombic $GaPO_4$ is relatively less open than that of orthorhombic $AlPO_4$. Hence, the phase transition for $GaPO_4$ occurs at much higher temperature as compared to that of $AlPO_4$. Due to similar reasons, the enthalpy of phase transition also increases gradually with increase in Ga^{3+} contents (Table 2). Thus, smaller the M–O–P bond angle or higher the difference in the M–O–P bond angle between the orthorhombic and cubic lattice show higher values of transformation temperature and enthalpy of phase transition.

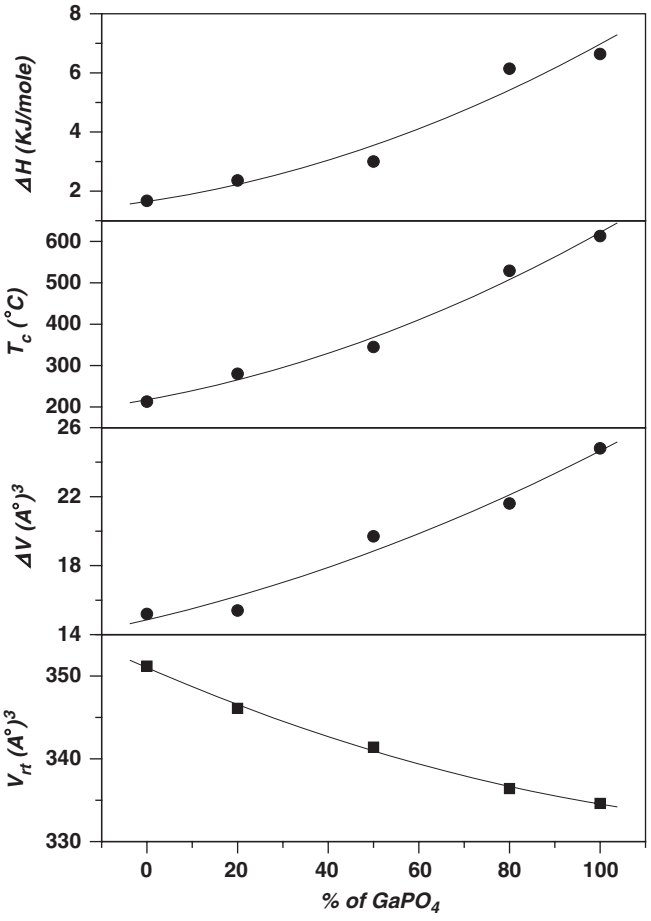

Fig. 8. Variation of transition temperature, enthalpy of phase transition, change in unit cell volume (excess volume) at transition temperature with composition for $Al_{1-x}Ga_xPO_4$.

It may be further added here that in a group-subgroup related displacive phase transitions, the transition behaviors are related to order parameters and lattice strains [35,36,40–45]. In such cases the strain in the low symmetric lattice is introduced as it transformed from a higher symmetric lattice. The larger the strain introduced the higher is the transformation temperature. In the present studied systems, the cubic high-cristobalite lattice transforms to orthorhombic low symmetric lattice on cooling the samples. The typical variations of strain with temperature for representative end members are shown in Fig. 9. The spontaneous strain parameters gradually decrease with temperature up to the phase transition temperature. A sharp decrease in spontaneous strain at the phase transition temperature supports the first order nature of the transformation. The principle strain e_{11}, e_{22} and e_{33} for the orthorhombic to cubic transformation in cristobalite lattice (between 25 °C and transition temperature) for different compositions are given in Table 3. It needs to mention here that in the formation of solid solution, the internal strain introduced due to the mismatch in the ionic radii. A comparison of various values of strain parameters for the cubic (high cristobalite) and orthorhombic (low cristobalite) transformation shows that a significant strain is introduced when Al^{3+} ion is substituted by Ga^{3+}. Similarly, the excess volume (ΔV, Table 2) at the phase transition temperature is maximum for $GaPO_4$ and minimum for $AlPO_4$. Such variation of internal strain of the solid solutions compositions often lead to a gradual variation in the phase transition temperature [43–46]. The further detail characterizations of the strain and order parameters are being carried out in these compositions. Also, the high-temperature studies of the intermediate

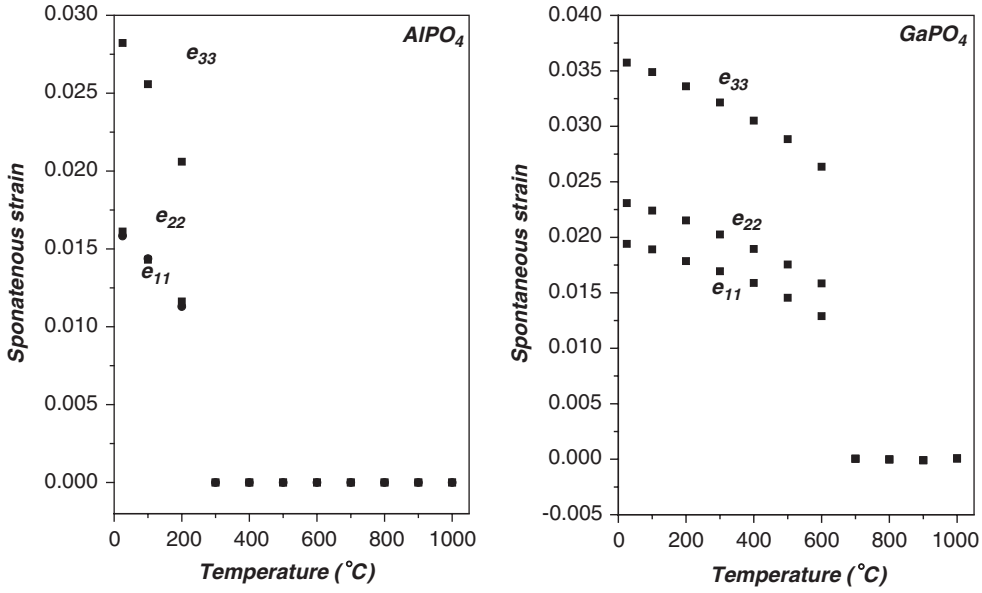

Fig. 9. Variation of spontaneous strain of $AlPO_4$ and $GaPO_4$ with temperature.

Table 3
Spontaneous strain parameters in low- and high-cristobalite structural transformation in $Al_{1-x}Ga_xPO_4$

S. no.	Sample	e_{11}	e_{22}	e_{33}	e_v
1	$AlPO_4$				
	(25–300 °C)	0.016	0.016	0.028	0.060
	(25 °C)[a]	0.016	0.016	0.029	0.061
2	$Al_{0.8}Ga_{0.2}PO_4$				
	(25–300 °C)	0.016	0.016	0.030	0.062
3	$Al_{0.5}Ga_{0.5}PO_4$				
	(25–400 °C)	0.018	0.020	0.034	0.072
4	$Al_{0.2}Ga_{0.8}PO_4$				
	(25–600 °C)	0.022	0.025	0.038	0.085
5	$GaPO_4$				
	(25–700 °C)	0.028	0.032	0.045	0.0105
	(25 °C)*	0.019	0.023	0.036	0.078

[a]Values obtained by extrapolating the high-temperature values to ambient temperature.

compositions as well as compositions close to the end member are in progress and will be communicated subsequently.

4. Conclusions

From the results reported in this study the formation of solid solution between $AlPO_4$ and $GaPO_4$ and the phase transformation between the low- and high-cristobalite phase has been established. The values of phase transition temperatures and the enthalpy of phase transition gradually increase with increasing Ga^{3+} contents for $Al_{1-x}Ga_xPO_4$ compositions. The phase transition temperature and the enthalpy of phase transition depend on the inter-polyhedral angle and the difference in the unit cell volume of the low- and high-cristobalite lattices as well as strain in the lattice. The high-cristobalite $GaPO_4$ slowly relaxes to trigonal quartz-type phase above 700 °C which on further heating retransforms to the high-cristobalite form above 960 °C. This high cristobalite to quartz phase transformation can be inhibited by partial substitution of Ga^{3+} by Al^{3+}.

References

[1] J.S.O. Evans, T.A. Mary, A.W. Sleight, J. Solid State Chem. 133 (1997) 580.
[2] J.S.O. Evans, T.A. Mary, T. Vogt, M.A. Subramanian, A.W. Sleight, Chem. Mater. 8 (1996) 2809.
[3] T.G. Amos, A.W. Sleight, J. Solid State Chem. 160 (2001) 230.
[4] P.M. Forster, A.W. Sleight, Int. J. Inorg. Mater. 1 (1999) 123.
[5] M.J. Burger, Am. Minerol. 33 (1948) 751.
[6] F.A. Hummel, J. Am. Ceram. Soc. 32 (1949) 320.
[7] W.R. Beck, J. Am. Ceram. Soc. 32 (1949) 147.
[8] A. Perloff, J. Am. Ceram. Soc. 39 (1956) 83.
[9] E. Schaffer, R. Roy, J. Am. Ceram. Soc. 39 (1956) 330.
[10] H. Sowa, Z. Kristallogr. 209 (1994) 954.
[11] O. Baumgartner, A. Preisinger, P.W. Krempl, H. Mang, Z. Kristallogr. 168 (1984) 83.
[12] A. Goiffon, J.C. Jumas, M. Maurin, E. Philippot, J. Solid State Chem. 61 (1986) 384.
[13] H. Nakae, K. Kihara, M. Okuno, S. Hirano, Z. Kristallogr. 210 (1995) 746.
[14] Y. Muraoka, K. Kihara, Phys. Chem. Min. 24 (1997) 243.
[15] J. Haines, O. Cambon, Z. Kristallogr. 219 (2004) 314.
[16] J. Haines, O. Cambon, R. Astier, P. Fertey, C. Chateau, Z. Kristallogr. 219 (2004) 32.
[17] J. Haines, O. Cambon, D. Cachau-Herreillat, G. Fraysse, F.E. Mallassagne, Solid State Sci. 6 (2004) 995.
[18] R.C.L. Mooney, Acta Crystallogr. 9 (1956) 728.
[19] S.K. Kulshreshtha, O.D. Jayakumar, V. Sudarshan, J. Phys. Chem. Solids 65 (2004) 1141.
[20] S.N. Achary, O.D. Jayakumar, A.K. Tyagi, S.K. Kulshreshtha, J. Solid State Chem. 176 (2003) 37.
[21] J.L. Robeson, R.R. Winter, W.S. Hammack, Phys. Rev. Lett. 73 (1994) 1644.

[22] J. Haines, O. Cambon, N. Prudhomme, G. Fraysse, Phys. Rev. B 73 (2006) 014103.
[23] P. Worsch, B. Koppenlhuber-Bitschnau, F.A. Mautner, P.W. Krempl, W. Wallnofer, Mater. Sci. Forum 278–281 (1998) 600.
[24] P. Worsch, B. Koppenlhuber-Bitschnau, F.A. Mautner, P.W. Krempl, W. Wallnofer, P. Doppler, J. Gautsch, Mater. Sci. Forum 312–324 (2000) 914.
[25] K. Kosten, H. Arnold, Z. Kristallogr. 152 (1980) 119.
[26] K. Jacobs, P. Hofmann, D. Klimm, J. Reichow, M. Schneider, J. Solid State Chem. 149 (2000) 180.
[27] H.N. Ng, C. Calvo, Can. J. Phys. 55 (1977) 677.
[28] D.M. Hatch, S. Ghose, J.L. Bjorkstam, Phys. Chem. Min. 21 (1994) 67.
[29] S.N. Achary, A.K. Tyagi, S.K. Kulshreshtha, O.D. Jayakumar, P.S.R. Krishna, A.B. Shinde, K.R. Chakraborty, Powder Diff. 20 (2005) 207.
[30] S.N. Achary, A.K. Tyagi, P.S.R. Krishna, A.B. Shinde, O.D. Jayakumar, S.K. Kulshresththa, Mater. Sci. Eng. B 123 (2005) 149.
[31] J. Rodriguez-Caravajal, Satellite Meeting on Powder Diffraction, in: Proceedings of the Fifteenth Conference of the International Union of Crystallography, Toulouse, France, vol. 127, 1990.
[32] JCPDS-11-500.
[33] D.C. Palmer, L. Finger, R.J. Hemley, R.T. Downs, in: Proceeding of the International Union of Crystallography, High-Pressure Group Meeting, May 30–31, 1992.
[34] G.P. Zheng, J.X. Zhang, J. Phys.: Condens. Matter 10 (1998) 275.
[35] H.-C. Freiheit, Solid State Commun. 119 (2001) 539.
[36] S. Marais, V. Heine, C. Nex, E. Salje, Phys. Rev. Lett. 66 (1991) 2480.
[37] P.F. Schofield, S.A.T. Redfern, J. Phys.: Condens. Matter 4 (1992) 375.
[38] M.A. Carpenter, A.I. Becerro, F. Seifert, Am. Mineral. 86 (2001) 348.
[39] D.C. Palmer, L.W. Finger, Am. Mineral. 79 (1994) 1.
[40] R. Ellemann-Olesen, T. Malcherek, Am. Mineral. 90 (2005) 1325.
[41] S. Qin, A.I. Becerro, F. Seifert, J. Gottsmann, J. Jiang, J. Mater. Chem. 10 (2000) 1609.
[42] R.J. Hemley, J. Shu, M.A. Carpenter, J. Hu, H.K. Mao, K.J. Kingma, Solid State Commun. 114 (2000) 527.
[43] E.K.H. Salje, Eur. J. Mineral. 7 (1995) 791.
[44] E.K.H. Salje, Phase Transitions in Ferroelastic and Co-elastic Crystals, Cambridge University Press, Cambridge, 1990.
[45] E. Salje, U. Bismayer, B. Wruck, J. Hensler, Phase Trans. 35 (1991) 61.
[46] S.N. Achary, A.K. Tyagi, J. Solid State Chem. 177 (2004) 3918.